*microbiology research*

MDPI

*Article*

# Evaluation of Predicted siRNA as an Antiviral against MERS-CoV Targeting the Membrane Gene in the Vero Cell Line

**Amany Y. El-Sayed [1,2,†], Mahmoud Shehata [1,3,*,†], Sara H. Mahmoud [1], Mahmoud ElHefnawi [4], Dina M. Seoudi [2] and Mohamed A. Ali [1,*]**

[1] Center of Scientific Excellence for Influenza Viruses, National Research Centre, Cairo 12622, Egypt; amanyamer13@gmail.com (A.Y.E.-S.); sarahussein9@yahoo.com (S.H.M.)
[2] Biochemistry Department, Faculty of Science, Ain Shams University, Cairo 11566, Egypt; dseoudi@sci.asu.edu.eg
[3] Institute of Medical Virology, JLU-Giessen University, 35390 Giessen, Germany
[4] Biomedical Informatics and Chemoinformatics Group, Informatics and Systems Department, National Research Centre, Cairo 12622, Egypt; mahef111@gmail.com
* Correspondence: shehata_mmm@hotmail.com (M.S.); mohamedahmedali2004@yahoo.com (M.A.A.)
† These authors contributed equally to this work.

**Abstract:** The Middle East respiratory syndrome coronavirus (MERS-CoV) was first isolated from a patient with acute pneumonia and renal failure in Saudi Arabia in 2012. By July 2023, MERS-CoV had resulted in 2605 human cases worldwide, causing a fatality rate of 36%, with 90.2% of cases being located in the Arabian Peninsula. The dromedary camel (*Camelus dromedarius*) is presumed to be an intermediate host for viral transmission to humans. So far, no prophylactic vaccines or effective antiviral treatments have been approved for MERS-CoV. RNA silencing is a novel approach for treating several diseases. A web-based bioinformatics tool (i-Score Designer) with integrative computational methods was used to predict and evaluate the designed siRNAs. This approach enabled the targeting of a highly conserved region of the MERS-CoV membrane (M) gene to inhibit virus replication. siRNA-M1, -M2, and -M3 were selected as the best of 559 designed siRNA candidates for an in vitro validation based on 2nd generation algorithm scoring, thermodynamic properties, off-target filtration, position-specific nucleotide preferences, and a free immune-stimulatory motifs. siRNAs were evaluated in Vero cells for their cytotoxicity and antiviral efficacy in vitro. Our results showed that the predicted siRNAs had no apparent cytotoxicity observed in Vero cells. The obtained results from the plaque reduction assay and RT-qPCR indicated that siRNA-M3 was the best candidate to inhibit MERS-CoV replication with a defined concentration of 400 picoMolar (pM). The computational methods used, and the in vitro evaluation, may provide an insight for a new antiviral strategy against MERS-CoV, a further in vivo study will nevertheless be required.

**Keywords:** siRNA; MERS-CoV; in silico; in vitro; antiviral



**Citation:** El-Sayed, A.Y.; Shehata, M.; Mahmoud, S.H.; ElHefnawi, M.; Seoudi, D.M.; Ali, M.A. Evaluation of Predicted siRNA as an Antiviral against MERS-CoV Targeting the Membrane Gene in the Vero Cell Line. *Microbiol. Res.* **2023**, *14*, 1687–1701. https://doi.org/10.3390/microbiolres14040116

Academic Editor: Takayuki Murata

Received: 4 September 2023
Revised: 11 October 2023
Accepted: 12 October 2023
Published: 17 October 2023



## 1. Introduction

MERS-CoV is a respiratory pathogen that emerged in June 2012 in Saudi Arabia in the case of a 60-year-old man patient who died of acute pneumonia and renal failure [1]. Since 2012, approximately 2605 human laboratory-confirmed cases of MERS-CoV infection have been reported in 27 countries, with 937 deaths, giving a case fatality rate of 36% [2]. MERS-CoV outbreaks were reported in the Arabian Peninsula, then circulated to more than 27 countries [3]. Phylogenetic analyses of camel and human isolates of the MERS-CoV genome showed that the viruses were highly identical [4,5]. Therefore, the single humped, dromedary camel (*Camelus dromedarius*) is considered as the main reservoir and primary source for virus transmission to humans [6,7]. MERS-CoV is an enveloped, single-strand positive-sense RNA virus with a genome length of approximately 30 kb that contains 11 open reading frames [8]. All RNA viruses can evade innate immune responses through

different strategies, mostly through the inhibition of type I interferon (IFN) production and IFN-mediated responses through viral proteins encoded in their genomes [9]. An in vitro study demonstrated that cyclosporin A inhibits MERS-CoV replication, and a treatment strategy using IFN-α has proven to be a successful approach for strongly inhibiting MERS-CoV replication 50–100 times more than SARS-CoV. This suggests that MERS-CoV expresses antagonist IFN proteins that influence viral pathogenicity [10]. The accessory proteins are strongly related to MERS-CoV pathogenicity as they interfere with host antiviral immune response through blocking one or more key signalling proteins in the IFN and NF-κB pathways, subsequently enhancing viral replication and pathogenesis [11–14].

Recently, two structural proteins, membrane (M) and nucleocapsid (N), have been shown to play a vital role in viral evasion of the immune response by suppressing interferon type-1 expression [15,16]. The MERS-CoV M protein acts as an interferon antagonist by suppressing RIG-I-induced activation of IFN regulatory factor 3 (IFR3), consequently inhibiting IFN expression [15]. Moreover, the M protein triggers apoptosis by activating the protein kinase R-like endoplasmic reticulum kinase (PERK) signalling pathway [17]. Therefore, the MERS-CoV M protein was approached as a promising therapeutic antigen for antibody production and other therapeutic strategies [18].

RNA interference (RNAi) is a specific post-transcriptional gene-silencing mechanism that is mediated by the small interfering RNA (siRNA) regulatory system [19]. siRNA silences gene expression by sequence-specific knockdown of the target mRNA using argonaute family proteins [20]. siRNA is a short nucleotide sequence about 21 to 23 nts in length, base paired with 2-nt 3′ overhangs for silencing gene expression of target mRNA. The guide siRNA strand was loaded into the RISC, forming active inducing RNA silencing complex [21,22]. Recently, three siRNA drugs (patisiran, givosiran, and lumasiran) were FDA approved for treatment for inherited genetic diseases [23,24].

Through in vivo study, C6G25S succeeded as a prophylactic and treatment approach by inhibiting the formation of infectious virion, consequently, the prevention of pulmonary alveolar damage, vascular thrombi, and immune cell infiltrations [25]. MERS-CoV ORF1ab expresses proteins for viral replication; therefore, it was selected as a promising target gene for in silico design of siRNA and miRNA against MERS-CoV [26]. Inhibition of viral replication has been observed in vitro and in vivo against multiple human viruses using RNAi approaches, such as SARS-CoV-2 [27], SARS-CoV [28], influenza virus [29,30], hepatitis C virus [31], human Papillomavirus [32], cytomegalovirus (CMV) [33], and other coronaviruses in vitro [34].

Hence, siRNA is a promising antiviral approach, as it is FDA approved for other diseases, has a low dosage, fewer side effects, is easily synthesized, is more specific and effective than either prophylactic or therapeutic approaches [35,36]. In our study, three siRNAs (siRNAs-M1, M2, and M3) designed against the highly conserved region of the MERS-CoV M gene were selected based on the scoring of second-generation algorithms of i-Score, S-biobredsi, and DSIR and other multistep filtrating approaches. The predicted siRNAs were synthesized chemically, and their cytotoxicity was evaluated in Vero cell lines. The siRNAs duplexes were validated for efficacy of replication inhibition against MERS-CoV in vitro.

## 2. Materials and Methods

### *2.1. In Silico Prediction*

#### 2.1.1. Sequences Collection, Alignments, and Analysis

MERS-CoV M gene sequences from different hosts and geographic regions were collected from the viral genome NCBI database (https://www.ncbi.nlm.nih.gov/genome/viruses/, accessed on 5 March 2021). To identify highly conserved regions in the viral RNA, M-gene sequence alignments were performed, then followed by conserved region analysis using BioEdit software (Version 7.2) [37].

2.1.2. Design, Prediction, and Selection of siRNA

The potent siRNAs were predicted, designed, and filtrated using web-based online software called i-Score Designer, whose algorithm is based on a linear regression model [38]. In addition to the i-Score Designer score, it evaluates nine different siRNA designing scores of first and second generation algorithms: Ui-Tei [39], Amarzguioui [40], Hsieh [41], Takasaki [42], s-Biopredsi [43], Reynolds [44], Katoh [45], composition and thermodynamics [46], DSIR [47], and calculates the ΔG value of the most stable secondary structure of an siRNA strand, dinucleotide ΔG value at 5′ and 3′ ends, the ΔG value throughout the siRNA stretch, the maximum length of GC stretches, and the GC% content [38]. As shown in Figure 1, the filtering process began with i-Score that based on the average threshold scores of second-generation algorithms (s-Biopredsi, i-Score, DSIR), and other significant thermodynamic parameters [48].

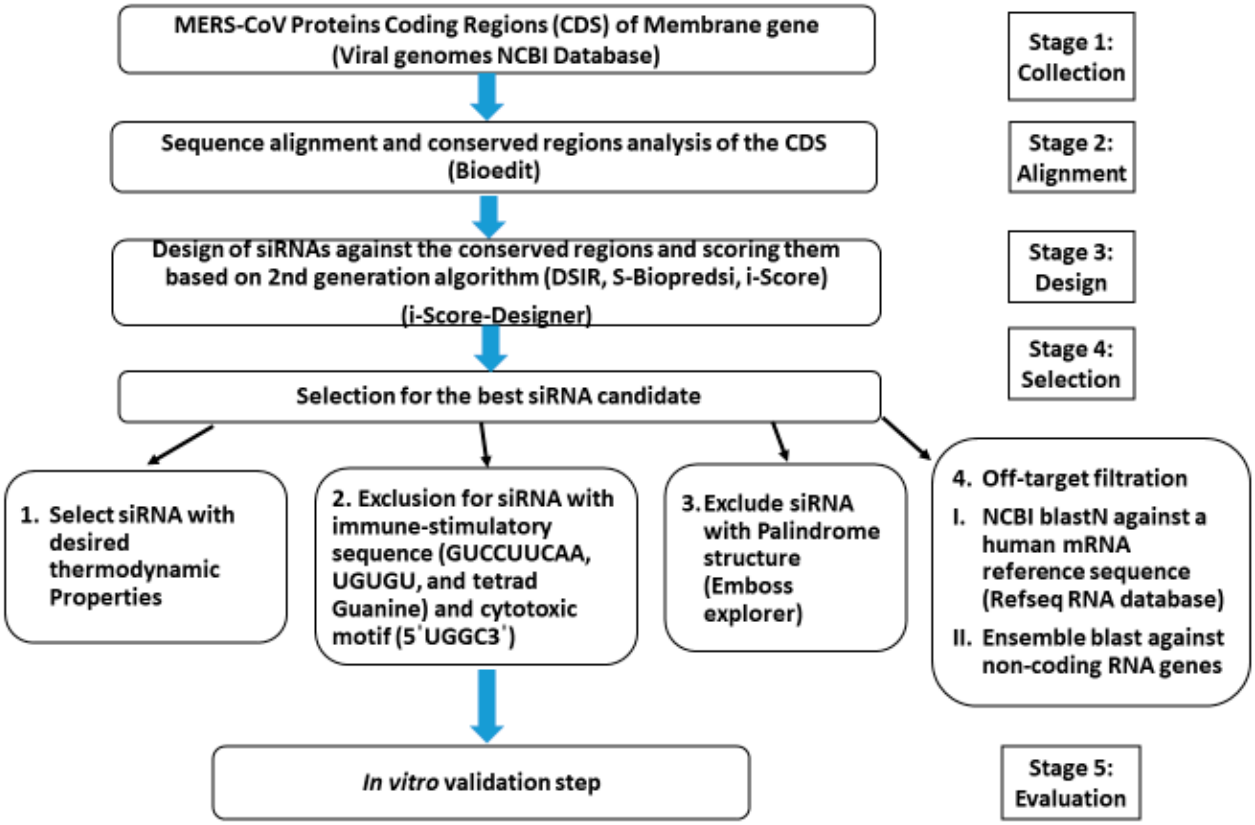


**Figure 1.** Workflow for the siRNAs in silico designing and selection steps targeting the MERS-CoV M-gene.

2.1.3. siRNAs Thermodynamic Properties

The i-Score software analysis is important in thermodynamics features such as the whole ΔG value, terminal dinucleotide thermodynamics, siRNA free energy, maximum length of GC stretch, and GC% content [38]. The final selection of the best candidate was based on two significant thermodynamic parameters, the whole ΔG value and GC% content. The unstable thermodynamics of siRNA were determined by the whole ΔG value of the siRNA secondary structure, desired to be $\geq -34$ Kcal/Mole as the coloration coefficient was proved to be more than 0.7 [38]. Then, the selection of the siRNA candidate was conducted with a GC content of approximately 36–53% [39,40,44]. Differential end instability at the 5′terminal end of the anti-sense strand is another selective parameter for potent siRNA candidates, as it affects the unwinding of the siRNA duplex, RISC-Complex formation, and target recognition [39]. Moreover, the asymmetrical base pairing rule determines the siRNA strand that acts as a guide strand and binds to the Ago protein of the RISC-

complex, which has the highest affinity towards uridine (U) at 5′end of the antisense strand. Hence, the guided strand is preferred to have A/U nucleotide at its 5′end in contrast to passenger strand with G/C nucleotide at its 5′end [49]. In addition, low internal stability (with low GC content) of the siRNA strand at the energy valley (position of ninth to the fourteenth nucleotides) is the most desirable conformation of the RISC complex during mRNA cleavage [50]. The emboss explorer was used to detect palindrome structures with more than 4 nucleotides to prevent formation of the secondary structure, which effects siRNA accessibility to target genes [51].

#### 2.1.4. Removal of Off-Target siRNAs

This is because the short length of the siRNA duplex is supposed to have multiple target transcripts, causing off-target gene silencing. Therefore, two filtration steps occur towards the selected siRNAs duplex (sense and antisense) to eliminate any candidate with near-complete and/or seed-matching off-target effects [52]. First, the selected siRNAs duplex was blasted against the human NCBI reference mRNA sequence database using the blastN tool (https://blast.ncbi.nlm.nih.gov/Blast.cgi, accessed on 15 March 2021). Second, the selected candidate from the first filtration was blasted against a non-coding region of the mRNA present in the ensemble 3′UTR database (http://www.ensembl.org/index.html, accessed on 15 March 2021), accessed on 15 March 2021. The blastN parameters used were for a short input sequence as siRNA and identifying short matches in the database are illustrated in Table 1 [53,54]. The successful candidate was with no complete or seed-matching homologus with mRNA. Many mRNA will have matching with the designed siRNA duplex but are not expressed in the targeted cell line, having no effect on the selection [52]. Some specific sequences must be excluded during siRNA design (5′UGUGU3′, 5′GUCCUUCAA3′, and tetrad Guanine), which provoke the immune response by binding to the toll-like receptor. In addition, the cytotoxic motif 5′UGGC3′ should be avoided in the siRNA sequence. A short siRNA length is preferred over the longest one as the later stimulates the innate immunity response [52,55].

**Table 1.** Parameter setup used for siRNA blastN analysis.

| Parameter | Value Setup Used |
|---|---|
| Word size | 7 |
| Expect threshold | 1000 |
| Match/Mismatch score | 1, −1 |
| Gap costs | 5, 2 |
| Maximum target sequence | 100 |
| Program selection | Somewhat similar sequences (blastN) |

#### 2.1.5. Final Selection and Chemical Synthesis

The selection for potential siRNAs was based on the guidelines and basic rules of filtration as described in the previously mentioned integrated bioinformatics methods, which are summarized in Figure 1. The selected siRNAs were chemically synthesized by the Eurofins company (Luxembourg) and used for further cytotoxicity and in vitro validation study.

### *2.2. In Vitro Evaluation*

#### 2.2.1. Cells and Virus

Vero cells (African Green Monkey Kidney cells, ATCC CCL-81) were grown in T-75 tissue culture flasks in Dulbecco's modified Eagle's medium (DMEM) containing a 10% foetal bovine serum (FBS) and 2% penicillin-streptomycin (pen/strep) mixture (Invitrogen, CA, USA). The cells were incubated for 24 h until confluency at 37 °C in a 5% $CO_2$ incubator for in vitro assays. The MERS-CoV (Dromedary/Egypt-NRCE-HKU270/2013), under accession number KJ477103, was inoculated in Vero cells maintained in DMEM media containing 2% FBS and 1% pen/strep at 37 °C in a 5% $CO_2$ incubator. Culture supernatant

samples were harvested and stored at −80 °C until the determining of viral titres using a plaque assay.

#### 2.2.2. Cytotoxicity Evaluation of siRNAs

Vero cells were used for in vitro evaluation of siRNA against MERS-CoV. Each lyophilized siRNA duplex was dissolved in a 5x universal SiMAX siRNA buffer to generate a storage stock at 100 pM/µL according to instructions from the product manual. Briefly, in a 96-well plate, 4 µL (400 pM) of each siRNA was bi-fold serially diluted quadruplicate in 110 µL of DMEM media containing 2% FBS and 1% pen/strep (Invitrogen, CA, USA). A total of 100 µL of each dilution were dispensed individually in 4-well plates and incubated for 72 h at 37 °C in a 5% $CO_2$ incubator. The untreated Vero cells were used as control cells. The cells' supernatants were discarded after 3 days followed by adding 20 µL of MTT reagent (5 mg/mL) in darkness, then the plates were incubated for 3 h at 37 °C in a 5% $CO_2$ incubator. During the incubation period, insoluble formazan crystals were formed, which were solubilized by 180 µL of 10% DMSO in $ddH_2O$. The absorbance of formazan solutions was measured at λmax 540 nm with 620 nm as a reference wavelength using a multi-well plate spectrophotometer. The obtained results were used to plot a graph of the cell-viability percentage against a log siRNAs concentration followed by determination of the half maximal cytotoxic concentration ($CC_{50}$).

#### 2.2.3. siRNA Transfection

The three siRNAs were transfected separately in triplicate into 6-well plates with a transfection dose of 400 pM for each, using transfecting agent Lipofectamine™ 3000 (Invitrogen, CA, USA). Briefly, the 400 pM siRNAs concentration was diluted in 50 µL Opti-MEM reduced serum medium (Thermo, MA, USA). A total of 10 µL of Lipofectamine reagent in 50 µL opti-MEM was incubated at room temperate for 5 min, followed by mixing an equal volume of each siRNA and Lipofectamine reagent, this was then incubated for 15 min at room temperature. Vero cells were maintained in 900 µL of free Opti-MEM media then the transfection mixtures were added in individual wells of a 6-well plate. Media were discarded after 6h of incubation at 37 °C in a 5% $CO_2$ humidified incubator, then the cells were ready for the next viral infection step. This experiment was repeated separately in triplicate for each siRNA (M1, M2, and M3).

#### 2.2.4. Evaluation of MERS-CoV Replication Inhibition in Transfected Vero Cells

The virus inoculation was performed post-transfection into the transfected Vero cell lines. Briefly, the siRNA-transfected Vero cells were infected with MERS-CoV (Dromedary/Egypt-NRCE-HKU270/2013) at a multiplicity of infection (MOI) of 0.005 for a 1 h incubation. The inoculum was discarded. Afterwards, DMEM media containing 2% FBS and 1% pen/strep were added and incubated for 48 h at 37 °C in a 5% $CO_2$ humidified incubator. A total of 200 µL of the cell supernatants were collected in triplicate at 12, 24 and 48 h post-infection (h p.i.) for each siRNA (M1, M2, M3). The samples were stored at −80 °C until used for viral quantification by plaque assay followed by purification of viral RNA and RT-qPCR of viral upE-gene [56,57]. The untreated control was Vero cells infected with MERS-CoV.

#### 2.2.5. Plaque Assay for Viral Titer Determination

A plaque assay was performed to determine the viral titer after cell treatment by siRNAs. Briefly, the collected supernatant samples at 12, 24, and 48 h p.i. were diluted in 10-fold dilution from $1{:}10^{-1}$ to $1{:}10^{-8}$ in DMEM media containing 2% FBS and 1% Pen/Strep. Afterwards, 100 µL of each dilution was inoculated into three individual wells of 12-well tissue culture plates with a confluent Vero cells monolayer maintained in 200 µL infection media and incubated at 37 °C for 1 h in a humidified incubator with 5% $CO_2$. The inoculum was removed gently from the infected monolayer cells after 1 h then the monolayer cells were overlaid with 1× MEM media containing 1% agar and 1% Pen/Strep.

The plates were left to solidify and incubated at 37 °C in humidified incubator with 5% $CO_2$ for 72 h upside down until the formation of viral plaques were visible. The cells were fixed with 3.4% formaldehyde solution for 1 h at RT. The plaque formed was visualized by staining cells with 1% crystal violet solution (in 20% methanol) for 30 min at RT then washed with water. Then, the following equation was used to calculate the viral titre reduction percentage [57].

$$\% \text{ of plaque reduction} = \frac{\text{virus control plaques count} - \text{sample plaques count}}{\text{virus control plaques count}} \times 100$$

2.2.6. Total RNA Extraction and Real-Time PCR

The cell supernatants of time post-infection (24 h and 48 h) for the treated and the untreated cells with siRNAs were isolated for viral RNA extraction using a KingFisher™ Flex Magnetic Particle Processor with a 96 Deep-Well Head according to the manufacturer's instructions (Thermo, MA, USA). The purified RNA was further used for a real-time quantitative polymerase chain reaction (RT-qPCR) targeting upstream MERS-CoV E-gene using an Eppendorf Real-Time PCR System and a verso one-Step RT-PCR Kit (Thermo, MA, USA) [56]. Briefly, a total 25 µL of PCR reaction containing 5 µL of RNA, 12.5 µL of 2× reaction buffer, 0.25 µL of enzyme mixture from the kit, 1.25 µL of enhancer, 3.5 µL $ddH_2O$, 1 µL of 10 µM concentrations of each upE forward primer (GCAACGCGCGATTCAGTT), reverse primer (GCCTCTACACGGGACCCATA), and 0.5 µL of 10 µM concentration of an upE probe (FAM-CTCTTCACATAATCGCCCCGAGCTCG-TAMRA). Thermal cycling involved 50 °C for 15 min, followed by 95 °C for 15 min, and then 45 cycles of 95 °C for 15 s and 60 °C for 60 s. Plasmid containing partial E fragment was used as a standard to calculate the viral load (copies/µL). All the experimental methods are summarized in Figure 2.

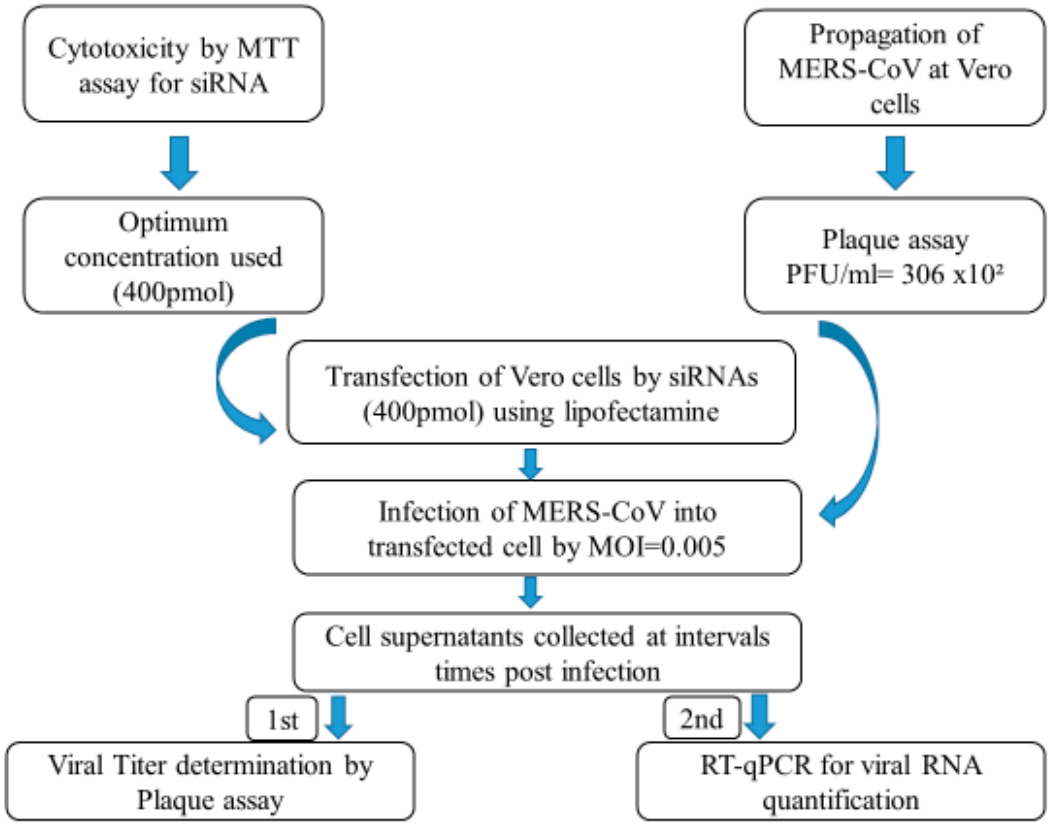


**Figure 2.** A flowchart for in vitro experimental methods to evaluate siRNA efficacy against MERS-CoV replication.

## 3. Results

### *3.1. In Silico Scoring, Prediction, and Selection of Potent siRNAs*

The collected sequences from the NCBI Database were used as a platform for siRNA design against the MERS-CoV M-gene. After performing multiple sequence alignment for the nucleotide coding sequences of the (M) gene, followed by conserved regions analysis using BIOEDIT software, our results showed that the m-gene had five conserved regions among all the collected isolates as shown in the alignment Figure 3. The i-Score Designer was used for designing and scoring of potential siRNAs. The five conserved regions of the M-gene were used as an input for the i-Score which generated about 559 siRNA candidates against these conserved regions. In Table 2, out of the 559 siRNAs, three siRNA (M1, M2, M3) candidates were selected based on their second-generation algorithm score, thermodynamic properties, off-target filtration, base preference, and other guideline rules. The integrative computational methods proposed that the three siRNAs may induce silencing effects on the MERS-CoV M-gene.

**Figure 3.** Multiple sequence alignments for the M-gene coding region for selected MERS-CoV sequences.

**Table 2.** List of predicated universal siRNAs against the MERS-CoV membrane (M) gene.

| Targeted Conserved Regions/(siRNA Name) | Pos. in the Genome | Sense Strand (5′→3′) | Antisense Strand (5′→3′) | Whole ΔG | GC % | DSIR | i-SCORE | s-Biopredsi |
|---|---|---|---|---|---|---|---|---|
| 2 (M1) | 206 to 359 | GAUAAU-CUCUGG-CAUUGUA | UACAAU-GCCAGA-GAUUAUCug | −34.3 | 6.8 | 95.2 | 73.8 | 0.869 |
| 3 (M2) | 368 to 437 | UAACUG-CUGUUG-UAACCAA | UUGGUU-ACAACA-GCAGUUAca | −34.3 | 36.8 | 83.6 | 63.6 | 0.757 |
| 4 (M3) | 439 to 464 | AAAAUG-GCUGGC-AUGCAUU | AAUGCA-UGCCAG-CCAUUUUga | −36.3 | 42.1 | 68.1 | 52.3 | 0.631 |

Figure 4 illustrates the output of each filtration step. From a total 494 MERS-CoV M-gene sequences, five conserved regions were analysed by the i-SCORE database. Afterwards, 28 siRNA were selected using 2nd generation algorithms. As a final output, three potent siRNAs (M1, M2, and M3) were selected. These three siRNAs were checked for cytotoxicity and in vitro antiviral screening against MERS-CoV in Vero cells.

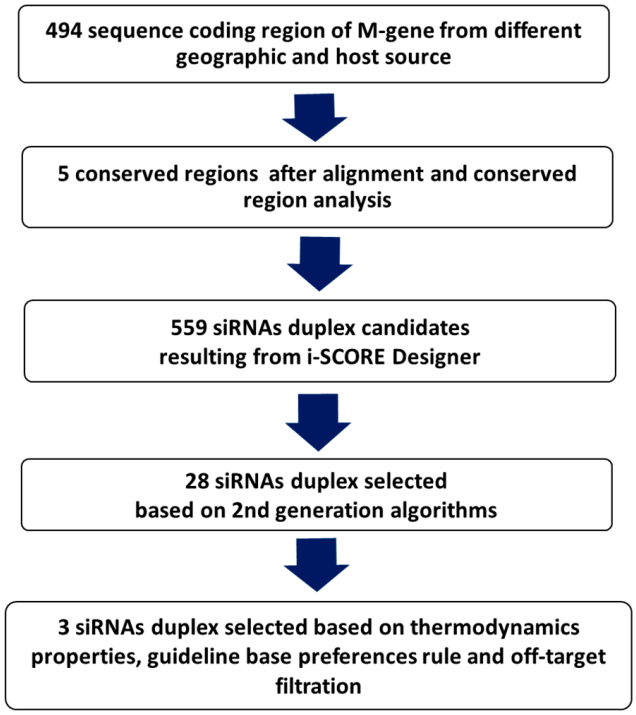


**Figure 4.** In silico filtration step outputs.

### *3.2. Cytotoxicity and Transfection*

The cytotoxic effect of selected siRNAs on the Vero cells' viability percentage is shown in Figure 5. The results indicated that there was no significant cytotoxicity on Vero cells as the half maximal cytotoxic concentration ($CC_{50}$) for siRNA-M1 = 804.6 picomolar (pM), siRNA-M2 = 549.9 pM, and siRNA-M3 = 903.5 pM. The Vero cells were transfected with the three siRNAs with a safe concentration below the $CC_{50}$ concentration = 400 pM. All the experiments were performed in triplicate for each siRNA and analysed using GraphPad prism software.

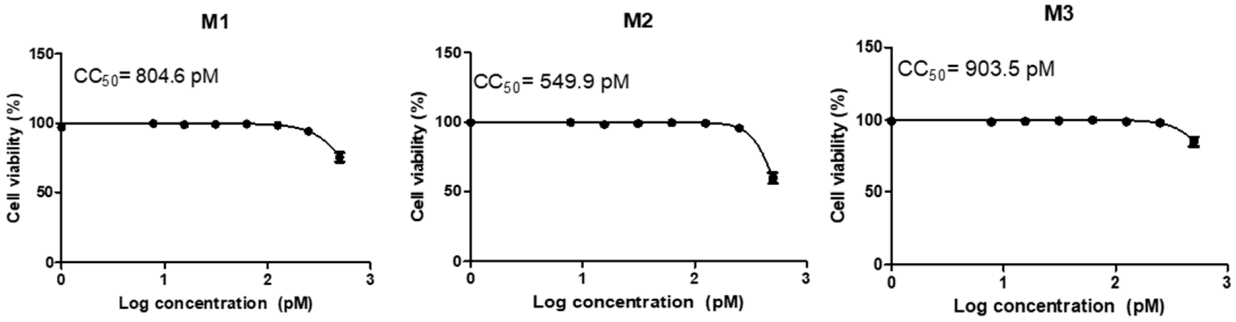


**Figure 5.** Schematic graphs for the cytotoxicity of selected siRNAs (M1, M2, and M3) in Vero cells.

### *3.3. Evaluation of MERS-CoV Replication Inhibition by Plaque Assay*

A plaque assay was performed to determine the titer of infectious virus after treatment with the three siRNAs. The cell supernatants of treated and untreated cells by siRNAs were inoculated at different concentrations (serially 10-fold diluted) for 1h. Figure 6 and

Table 3 show the viral titres for each sample taken at different time points post-infection and the reduction percentage for different siRNAs on MERS-CoV replication were calculated. The results showed that the inhibition of viral replication was variable among the three siRNAs. The siRNA-M3 showed a significant reduction in viral titre at 24 and 48 h post-infection (h p.i.) with a reduction percentage of 83.6% and 91%, respectively, in comparison with untreated control cells. Over time the siRNA-M2 had an insignificant effect on viral replication. At 48 h p.i., siRNA-M1 had a considerably significant reduction in viral titre by 80.5% inhibition, compared with the untreated control. We can conclude that siRNA-M1 and siRNA-M3 have a significant reduction percent of MERS-CoV inhibition after 48 h p.i. as shown in Table 3.

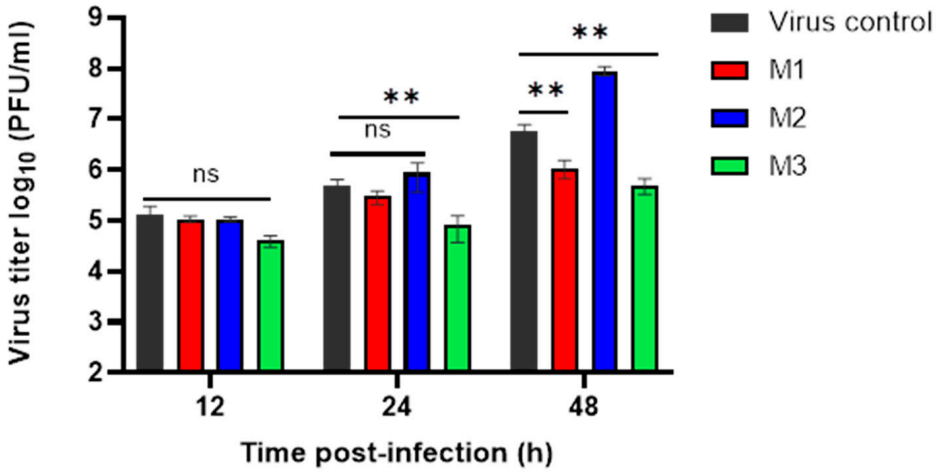


**Figure 6.** Graphical representation for viral titres ($log_{10}$PFU/mL) after siRNA (M1, M2, and M3) treatment with a concentration of 400 pM at different time points post-infection with MERS-CoV. Vero cells were transfected with siRNAs (M1, M2, M3). Afterwards, Vero cells infected with MERS-CoV (MOI = 0.005) at 24 h post-transfection, then cells supernatants were collected in-triplicate at 12, 24 and 48 h post-infection (h p.i.) for each siRNA. The significant differences are indicated (** = $p < 0.01$, and non-significant = ns).

**Table 3.** Viral titer reduction percentage at different times after treatment with the three siRNAs in Vero cells.

| Time Post Infection (h) | Viral Titer Reduction of M1 (%) | Viral Titer Reduction of M2 (%) | Viral Titer Reduction of M3 (%) |
|---|---|---|---|
| 12 | 20 | 20 | 70 |
| 24 | 39.45 | −76.87 | 83.67 * |
| 48 | 80.58 * | −1488.23 | 91.17 * |

* Refers to the fact that if the viral reduction inhibition percentage was more than 75%, there was a significant effect.

### *3.4. Evaluation of MERS-CoV Replication by RT-qPCR*

This result of the RT-qPCR was a confirmatory assay for the plaque reduction results after treating cells with different siRNAs. The cell culture supernatant of treated and untreated cells with siRNAs were collected at 24 and 48 h p.i. in triplicate. Viral RNA was extracted from cells supernatants followed by RT-qPCR analysis targeting the MERS-CoV up-stream E-gene (upE). In Figure 7, there was a highly significant reduction in the RNA copy number of viral samples taken after 48 h p.i. of treated cells by siRNA-M3, in comparison with the untreated virus-infected cells. siRNA-M1 and M2 showed insignificant reductions in the RNA copy number, compared with the untreated control after 24 and 48 h p.i.

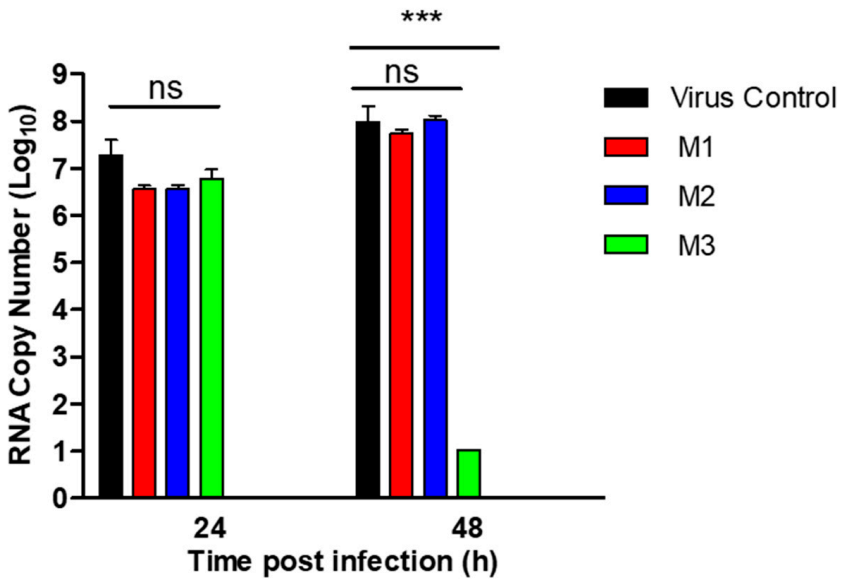


**Figure 7.** A graphical representation for the RNA copy number of collected samples after 24 and 48 h post-infection with MERS-CoV in Vero cells treated with a concentration 400 pM of the three siRNAs (M1, M2, and M3). Vero cells were transfected with siRNAs (M1, M2, M3). Afterwards, Vero cells were infected with MERS-CoV (MOI = 0.005) at 24 h post-transfection, then the cells supernatants were collected in triplicate at 24 and 48 h p.i. for each siRNA. The significant differences are indicated (*** = $p < 0.001$ and non-significant = ns).

## 4. Discussion

The first identified case of MERS-CoV was in Saudi Arabia in 2012, resulting in death with multi-organ failure and acute pneumonia [1]. In the meantime, MERS-CoV became a public health concern as 27 different countries have reported human infections with a case fatality rate of 36% [2]. The single-humped, dromedary camel has been identified as the intermediate host for MERS-CoV human transmission [7,58,59]. The phylogenetic analysis of human and camel MERS-CoV isolates estimated that the virus genome is divided into three major clades, known as clades A, B, and C [60].

Several hypothesis demonstrated the potential risk of camel-to-human MERS-CoV transmission through airborne contact with infected dromedary camels [6], saliva, nasal secretions during slaughtering, involvement in camel training, and milking camels [61], using unpasteurized camel milk, raw meat, viscera, and/or medicinal use of camel urine [62]. Five species, the European hedgehog, two species of bats, the dromedary camel, and humans have been reported with MERS-CoV infections [63].

Dipeptidyl peptidase 4 (DPP4) is the functional receptor for the receptor-binding S1 domain (RBD) of the MERS-CoV spike protein [64]. By alignment of DPP4 sequences of various domestic mammalian species, it showed identically in the DPP4 residues among different species. This indicates the sustainability of these species to MERS-CoV infection from which infection can spill over to humans [60,65]. The seroprevalence of MERS-CoV specific antibodies and viral detection of MERS-CoV in investigated camels and people exposed to camels from different countries indicated the high risk of camel traders, abattoir workers, and camel workers (regularly involved in the training or herding of camels, cleaning farm equipment, and milking camels) to MERS-CoV infections [66–69].

Until now, no specific therapy against MERS-CoV infection has been available as the infected cases receive a supportive treatment based on their clinical condition [70]. Repurposing old drugs against MERS-CoV may offer a survival advantage but not with all cases [71]. Therefore, vaccines and new treatments against MERS-CoV infection were highly needed. RNAi technology has recently been approved for treatment against several diseases and pathogenic infections, though siRNAs were targeted their complementary

mRNA degradation [72]. In our study, the integrative computational methods proposed that the three siRNAs may induce a silencing effect on the MERS-CoV M gene, based on the analysis parameters showed in Table 2. This is comparable to one of the effective studies that showed that SARS-CoV-2 infection was suppressed by the mRNA of RdRp through siRNA therapy [73].

Here, we evaluated the efficacy of designed siRNAs against the M gene of MERS-CoV replication in Vero cells. Three siRNAs (siRNAs-M1, M2, and M3) out of 559 candidates were selected as having the most promising anti-MERS-CoV activity. siRNAs-M1 and M3 showed a significant reduction in viral titres at 48 h p.i. compared with the untreated control cells. The efficacy of siRNAs has been reported for the inhibition of other coronaviruses in vitro [34]. The RNA level of siRNA-M1 showed no significant difference compared to the control after 24 and 48 h p.i., as illustrated in Figure 7. That these results are not comparable with viral titer reduction at the same time points in Figure 6, may be related to there being a reduction in the infectious viral particles and there still being a transcribed viral RNA found. The obtained results from our study confirmed a significant reduction in the RNA copy number of siRNA-M3 after 48 h p.i in comparison with the untreated virus control. These results were strengthened by a significant viral plaque reduction assay of siRNA-M3.

The accessory proteins (ORF3, ORF4a, ORF4b, ORF5 and ORF8b) and the two structure proteins M and N of MERS-CoV had been identified for their role in inhibiting the IFN signalling pathway through inhibition of the activation of the IFN-β promoter, the interferon stimulation response element (ISRE) promoter, and the transcription signalling factors necessary for interferon type I induction [12,16,74]. Also, various types of siRNAs were evaluated against HCV 5-NTR, and it was found that the HCV321, HCV353, HCV258 siRNAs were the best and most promising siRNAs for the inhibition of HCV replication [48].

The importance of the MERS-CoV M protein in viral pathogenicity was agreed with by studies by Lui et al. and Chu et al. [15,17] and used as a target for further therapeutic and prophylactic strategies [18]. The latest research has predicted that the ORF1a gene is a promising target site for siRNA predication, design and in vitro evaluation against MERS-CoV [75,76]. Our results highlighted the need to evaluate siRNA-M3 individually for its antiviral efficiency in animal models.

## 5. Conclusions

Therefore, our in silico prediction and filtration were essential steps before synthesis, which was used as antiviral treatment without off-targeting effects and increment of efficiency and specificity. Moreover, the in vitro evaluation of oligonucleotides by plaque viral reduction assay showed there are two siRNAs (M1 and M3) that inhibited the MERS-CoV replication after 48 h p.i. in Vero cells. The viral mRNA levels measured after treatment with different siRNAs showed that siRNA-M3 is the best candidate to be used as a therapeutic agent against MERS-CoV infection. Finally, viral diseases can be treated by the potential siRNAs and evaluated to produce novel antiviral therapeutics.

**Author Contributions:** Conceptualization, A.Y.E.-S., M.S., S.H.M., D.M.S. and M.A.A.; methodology, A.Y.E.-S., M.S. and S.H.M.; software, A.Y.E.-S., M.S. and S.H.M.; validation, A.Y.E.-S., M.S., S.H.M. and M.A.A.; data curation, A.Y.E.-S., M.S., D.M.S. and S.H.M.; supervision, M.S., D.M.S. and M.A.A.; writing—original draft preparation, A.Y.E.-S., M.S. and S.H.M.; writing—review and editing, All authors; funding acquisition, M.S. and M.A.A. All authors have read and agreed to the published version of the manuscript.

**Funding:** This research was funded by the National Research Centre, Internal project ID: 12020108, and the Academy of Scientific Research and Technology, project ID: 7182, Egypt. Moreover, M.S. was funded by the Alexander-von-Humboldt Foundation, Georg Forster research fellowship.

**Institutional Review Board Statement:** All experiments involving MERS-CoV were performed using Biosafety 3 laboratories provided by the local authorities at the National Research Centre (NRC), Egypt.

**Informed Consent Statement:** Not applicable.

**Data Availability Statement:** The data existing in this study are available in the article.

**Conflicts of Interest:** The authors declare no conflict of interest. The funders had no role in the design of the study, analyses, or interpretation of data; in the writing of the manuscript; or in the decision to publish the results.

## References


1. Zaki, A.M.; van Boheemen, S.; Bestebroer, T.M.; Osterhaus, A.D.; Fouchier, R.A. Isolation of a novel coronavirus from a man with pneumonia in Saudi Arabia. *N. Engl. J. Med.* **2012**, *367*, 1814–1820. [CrossRef]
2. WHO. *Middle East Respiratory Syndrome, Report June 2023*; WHO: Geneva, Switzerland, 2023.
3. Rabaan, A.A.; Al-Ahmed, S.H.; Sah, R.; Alqumber, M.A.; Haque, S.; Patel, S.K.; Pathak, M.; Tiwari, R.; Yatoo, M.I.; Haq, A.U.; et al. MERS-CoV: Epidemiology, molecular dynamics, therapeutics, and future challenges. *Ann. Clin. Microbiol. Antimicrob.* **2021**, *20*, 8. [CrossRef] [PubMed]
4. Raj, V.S.; Farag, E.A.; Reusken, C.B.; Lamers, M.M.; Pas, S.D.; Voermans, J.; Smits, S.L.; Osterhaus, A.D.; Al-Mawlawi, N.; Al-Romaihi, H.E.; et al. Isolation of MERS coronavirus from a dromedary camel, Qatar, 2014. *Emerg. Infect. Dis.* **2014**, *20*, 1339–1342. [CrossRef] [PubMed]
5. Chu, D.K.; Poon, L.L.; Gomaa, M.M.; Shehata, M.M.; Perera, R.A.; Abu Zeid, D.; El Rifay, A.S.; Siu, L.Y.; Guan, Y.; Webby, R.J.; et al. MERS coronaviruses in dromedary camels, Egypt. *Emerg. Infect. Dis.* **2014**, *20*, 1049–1053. [CrossRef] [PubMed]
6. Azhar Esam, I.; Hashem Anwar, M.; El-Kafrawy Sherif, A.; Sohrab Sayed, S.; Aburizaiza Asad, S.; Farraj Suha, A.; Hassan Ahmed, M.; Al-Saeed Muneera, S.; Jamjoom Ghazi, A.; Madani Tariq, A. Detection of the Middle East Respiratory Syndrome Coronavirus Genome in an Air Sample Originating from a Camel Barn Owned by an Infected Patient. *mBio* **2014**, *5*, e01450-14. [CrossRef] [PubMed]
7. Perera, R.A.; Wang, P.; Gomaa, M.R.; El-Shesheny, R.; Kandeil, A.; Bagato, O.; Siu, L.Y.; Shehata, M.M.; Kayed, A.S.; Moatasim, Y.; et al. Seroepidemiology for MERS coronavirus using microneutralisation and pseudoparticle virus neutralisation assays reveal a high prevalence of antibody in dromedary camels in Egypt, June 2013. *Eurosurveillance* **2013**, *18*, 20574. [CrossRef]
8. Kandeil, A.; Shehata, M.M.; El Shesheny, R.; Gomaa, M.R.; Ali, M.A.; Kayali, G. Complete Genome Sequence of Middle East Respiratory Syndrome Coronavirus Isolated from a Dromedary Camel in Egypt. *Genome Announc.* **2016**, *4*, 10–1128. [CrossRef]
9. Basler, C.F.; Amarasinghe, G.K. Evasion of interferon responses by Ebola and Marburg viruses. *J. Interferon Cytokine Res.* **2009**, *29*, 511–520. [CrossRef]
10. De Wilde, A.H.; Raj, V.S.; Oudshoorn, D.; Bestebroer, T.M.; van Nieuwkoop, S.; Limpens, R.; Posthuma, C.C.; van der Meer, Y.; Bárcena, M.; Haagmans, B.L.; et al. MERS-coronavirus replication induces severe in vitro cytopathology and is strongly inhibited by cyclosporin A or interferon-α treatment. *J. Gen. Virol.* **2013**, *94*, 1749–1760. [CrossRef]
11. Menachery, V.D.; Mitchell, H.D.; Cockrell, A.S.; Gralinski, L.E.; Yount, B.L.; Graham, R.L.; McAnarney, E.T.; Douglas, M.G.; Scobey, T.; Beall, A.; et al. MERS-CoV Accessory ORFs Play Key Role for Infection and Pathogenesis. *mBio* **2017**, *8*, e00665-17. [CrossRef]
12. Wong, L.-Y.R.; Ye, Z.-W.; Lui, P.-Y.; Zheng, X.; Yuan, S.; Zhu, L.; Fung, S.-Y.; Yuen, K.-S.; Siu, K.-L.; Yeung, M.-L.; et al. Middle East Respiratory Syndrome Coronavirus ORF8b Accessory Protein Suppresses Type I IFN Expression by Impeding HSP70-Dependent Activation of IRF3 Kinase IKKε. *J. Immunol.* **2020**, *205*, 1564–1579. [CrossRef] [PubMed]
13. Shokri, S.; Mahmoudvand, S.; Taherkhani, R.; Farshadpour, F. Modulation of the immune response by Middle East respiratory syndrome coronavirus. *J. Cell. Physiol.* **2019**, *234*, 2143–2151. [CrossRef] [PubMed]
14. Lee, J.Y.; Bae, S.; Myoung, J. Middle East Respiratory Syndrome Coronavirus-Encoded Accessory Proteins Impair MDA5-and TBK1-Mediated Activation of NF-κB. *J. Microbiol. Biotechnol.* **2019**, *29*, 1316–1323. [CrossRef] [PubMed]
15. Lui, P.-Y.; Wong, L.-Y.R.; Fung, C.-L.; Siu, K.-L.; Yeung, M.-L.; Yuen, K.-S.; Chan, C.-P.; Woo, P.C.-Y.; Yuen, K.-Y.; Jin, D.-Y. Middle East respiratory syndrome coronavirus M protein suppresses type I interferon expression through the inhibition of TBK1-dependent phosphorylation of IRF3. *Emerg. Microbes Infect.* **2016**, *5*, e39. [CrossRef] [PubMed]
16. Chang, C.-Y.; Liu Helene, M.; Chang, M.-F.; Chang Shin, C. Middle East Respiratory Syndrome Coronavirus Nucleocapsid Protein Suppresses Type I and Type III Interferon Induction by Targeting RIG-I Signaling. *J. Virol.* **2020**, *94*, e00099-20. [CrossRef] [PubMed]
17. Chu, H.; Shuai, H.; Hou, Y.; Zhang, X.; Wen, L.; Huang, X.; Hu, B.; Yang, D.; Wang, Y.; Yoon, C.; et al. Targeting highly pathogenic coronavirus-induced apoptosis reduces viral pathogenesis and disease severity. *Sci. Adv.* **2021**, *7*, eabf8577. [CrossRef]
18. Park, B.K.; Lee, S.I.; Bae, J.-Y.; Park, M.-S.; Lee, Y.; Kwon, H.-J. Production of a Monoclonal Antibody Targeting the M Protein of MERS-CoV for Detection of MERS-CoV Using a Synthetic Peptide Epitope Formulated with a CpG–DNA–Liposome Complex. *Int. J. Pept. Res. Ther.* **2019**, *25*, 819–826. [CrossRef]
19. Elbashir, S.M.; Harborth, J.; Lendeckel, W.; Yalcin, A.; Weber, K.; Tuschl, T. Duplexes of 21-nucleotide RNAs mediate RNA interference in cultured mammalian cells. *Nature* **2001**, *411*, 494–498. [CrossRef]
20. Obbard, D.J.; Gordon, K.H.; Buck, A.H.; Jiggins, F.M. The evolution of RNAi as a defence against viruses and transposable elements. *Philos. Trans. R. Soc. B Biol. Sci.* **2009**, *364*, 99–115. [CrossRef]

21. Dana, H.; Chalbatani, G.M.; Mahmoodzadeh, H.; Karimloo, R.; Rezaiean, O.; Moradzadeh, A.; Mehmandoost, N.; Moazzen, F.; Mazraeh, A.; Marmari, V.; et al. Molecular Mechanisms and Biological Functions of siRNA. *Int. J. Biomed. Sci.* **2017**, *13*, 48–57. [CrossRef]
22. Mehta, A.; Michler, T.; Merkel, O.M. siRNA Therapeutics against Respiratory Viral Infections-What Have We Learned for Potential COVID-19 Therapies? *Adv. Healthc. Mater.* **2021**, *10*, 2001650. [CrossRef] [PubMed]
23. Holm, A.; Løvendorf, M.B.; Kauppinen, S. Development of siRNA Therapeutics for the Treatment of Liver Diseases. *Methods Mol. Biol.* **2021**, *2282*, 57–75. [CrossRef] [PubMed]
24. Scott, L.J.; Keam, S.J. Lumasiran: First Approval. *Drugs* **2021**, *81*, 277–282. [CrossRef] [PubMed]
25. Chang, Y.C.; Yang, C.F.; Chen, Y.F.; Yang, C.C.; Chou, Y.L.; Chou, H.W.; Chang, T.Y.; Chao, T.L.; Hsu, S.C.; Ieong, S.M.; et al. A siRNA targets and inhibits a broad range of SARS-CoV-2 infections including Delta variant. *EMBO Mol. Med.* **2022**, *14*, e15298. [CrossRef]
26. Nur, S.M.; Hasan, M.A.; Amin, M.A.; Hossain, M.; Sharmin, T. Design of Potential RNAi (miRNA and siRNA) Molecules for Middle East Respiratory Syndrome Coronavirus (MERS-CoV) Gene Silencing by Computational Method. *Interdiscip. Sci. Comput. Life Sci.* **2015**, *7*, 257–265. [CrossRef]
27. Bowden-Reid, E.; Ledger, S.; Zhang, Y.; Di Giallonardo, F.; Aggarwal, A.; Stella, A.O.; Akerman, A.; Milogiannakis, V.; Walker, G.; Rawlinson, W.; et al. Novel siRNA therapeutics demonstrate multi-variant efficacy against SARS-CoV-2. *Antivir. Res.* **2023**, *217*, 105677. [CrossRef]
28. Li, T.; Zhang, Y.; Fu, L.; Yu, C.; Li, X.; Li, Y.; Zhang, X.; Rong, Z.; Wang, Y.; Ning, H.; et al. siRNA targeting the Leader sequence of SARS-CoV inhibits virus replication. *Gene Ther.* **2005**, *12*, 751–761. [CrossRef]
29. Jamali, A.; Mottaghitalab, F.; Abdoli, A.; Dinarvand, M.; Esmailie, A.; Kheiri, M.T.; Atyabi, F. Inhibiting influenza virus replication and inducing protection against lethal influenza virus challenge through chitosan nanoparticles loaded by siRNA. *Drug Deliv. Transl. Res.* **2018**, *8*, 12–20. [CrossRef]
30. ElHefnawi, M.; Hassan, N.; Kamar, M.; Siam, R.; Remoli, A.L.; El-Azab, I.; AlAidy, O.; Marsili, G.; Sgarbanti, M. The design of optimal therapeutic small interfering RNA molecules targeting diverse strains of influenza A virus. *Bioinformatics* **2011**, *27*, 3364–3370. [CrossRef]
31. Aljowaie, R.M.; Almajhdi, F.N.; Ali, H.H.; El-Wetidy, M.S.; Shier, M.K. Inhibition of hepatitis C virus genotype 4 replication using siRNA targeted to the viral core region and the CD81 cellular receptor. *Cell Stress Chaperones* **2020**, *25*, 345–355. [CrossRef]
32. Togtema, M.; Jackson, R.; Grochowski, J.; Villa, P.L.; Mellerup, M.; Chattopadhyaya, J.; Zehbe, I. Synthetic siRNA targeting human papillomavirus 16 E6: A perspective on in vitro nanotherapeutic approaches. *Nanomedicine* **2018**, *13*, 455–474. [CrossRef] [PubMed]
33. Balakrishnan, K.N.; Abdullah, A.A.; Bala, J.A.; Jesse, F.F.A.; Abdullah, C.A.C.; Noordin, M.M.; Mohd-Azmi, M.L. Immediately early 2 (IE-2) and DNA polymerase SiRNA as virus-specific antiviral against novel transplacental cytomegalovirus strain ALL-03 in vitro. *Infect. Genet. Evol.* **2021**, *90*, 104783. [CrossRef] [PubMed]
34. Sajid, M.I.; Moazzam, M.; Cho, Y.; Kato, S.; Xu, A.; Way, J.J.; Lohan, S.; Tiwari, R.K. siRNA Therapeutics for the Therapy of COVID-19 and Other Coronaviruses. *Mol. Pharm.* **2021**, *18*, 2105–2121. [CrossRef]
35. Qureshi, A.; Tantray, V.G.; Kirmani, A.R.; Ahangar, A.G. A review on current status of antiviral siRNA. *Rev. Med. Virol.* **2018**, *28*, e1976. [CrossRef]
36. Hu, B.; Zhong, L.; Weng, Y.; Peng, L.; Huang, Y.; Zhao, Y.; Liang, X.-J. Therapeutic siRNA: State of the art. *Signal Transduct. Target. Ther.* **2020**, *5*, 101. [CrossRef] [PubMed]
37. Hall, T.A. BioEdit: A user-friendly biological sequence alignment editor and analysis program for Windows 95/98/NT. *Nucleic Acids Symp. Ser.* **1999**, *41*, 95–98.
38. Ichihara, M.; Murakumo, Y.; Masuda, A.; Matsuura, T.; Asai, N.; Jijiwa, M.; Ishida, M.; Shinmi, J.; Yatsuya, H.; Qiao, S.; et al. Thermodynamic instability of siRNA duplex is a prerequisite for dependable prediction of siRNA activities. *Nucleic Acids Res.* **2007**, *35*, e123. [CrossRef] [PubMed]
39. Ui-Tei, K.; Naito, Y.; Takahashi, F.; Haraguchi, T.; Ohki-Hamazaki, H.; Juni, A.; Ueda, R.; Saigo, K. Guidelines for the selection of highly effective siRNA sequences for mammalian and chick RNA interference. *Nucleic Acids Res.* **2004**, *32*, 936–948. [CrossRef]
40. Amarzguioui, M.; Prydz, H. An algorithm for selection of functional siRNA sequences. *Biochem. Biophys. Res. Commun.* **2004**, *316*, 1050–1058. [CrossRef]
41. Hsieh, A.C.; Bo, R.; Manola, J.; Vazquez, F.; Bare, O.; Khvorova, A.; Scaringe, S.; Sellers, W.R. A library of siRNA duplexes targeting the phosphoinositide 3-kinase pathway: Determinants of gene silencing for use in cell-based screens. *Nucleic Acids Res.* **2004**, *32*, 893–901. [CrossRef]
42. Takasaki, S.; Kotani, S.; Konagaya, A. An effective method for selecting siRNA target sequences in mammalian cells. *Cell Cycle* **2004**, *3*, 790–795. [CrossRef]
43. Huesken, D.; Lange, J.; Mickanin, C.; Weiler, J.; Asselbergs, F.; Warner, J.; Meloon, B.; Engel, S.; Rosenberg, A.; Cohen, D.; et al. Design of a genome-wide siRNA library using an artificial neural network. *Nat. Biotechnol.* **2005**, *23*, 995–1001. [CrossRef] [PubMed]
44. Reynolds, A.; Leake, D.; Boese, Q.; Scaringe, S.; Marshall, W.S.; Khvorova, A. Rational siRNA design for RNA interference. *Nat. Biotechnol.* **2004**, *22*, 326–330. [CrossRef] [PubMed]

45. Katoh, T.; Suzuki, T. Specific residues at every third position of siRNA shape its efficient RNAi activity. *Nucleic Acids Res.* **2007**, *35*, e27. [CrossRef]
46. Shabalina, S.A.; Spiridonov, A.N.; Ogurtsov, A.Y. Computational models with thermodynamic and composition features improve siRNA design. *BMC Bioinform.* **2006**, *7*, 65. [CrossRef] [PubMed]
47. Vert, J.-P.; Foveau, N.; Lajaunie, C.; Vandenbrouck, Y. An accurate and interpretable model for siRNA efficacy prediction. *BMC Bioinform.* **2006**, *7*, 520. [CrossRef] [PubMed]
48. ElHefnawi, M.; Kim, T.; Kamar, M.A.; Min, S.; Hassan, N.M.; El-Ahwany, E.; Kim, H.; Zada, S.; Amer, M.; Windisch, M.P. In silico design and experimental validation of siRNAs targeting conserved regions of multiple hepatitis C virus genotypes. *PLoS ONE* **2016**, *11*, e0159211. [CrossRef]
49. Frank, F.; Sonenberg, N.; Nagar, B. Structural basis for 5′-nucleotide base-specific recognition of guide RNA by human AGO2. *Nature* **2010**, *465*, 818–822. [CrossRef]
50. Khvorova, A.; Reynolds, A.; Jayasena, S.D. Functional siRNAs and miRNAs Exhibit Strand Bias. *Cell* **2003**, *115*, 209–216. [CrossRef]
51. Rice, P.; Longden, I.; Bleasby, A. EMBOSS: The European Molecular Biology Open Software Suite. *Trends Genet.* **2000**, *16*, 276–277. [CrossRef]
52. Mysara, M.; Garibaldi, J.M.; ElHefnawi, M. MysiRNA-designer: A workflow for efficient siRNA design. *PLoS ONE* **2011**, *6*, e25642. [CrossRef] [PubMed]
53. Birmingham, A.; Anderson, E.; Sullivan, K.; Reynolds, A.; Boese, Q.; Leake, D.; Karpilow, J.; Khvorova, A. A protocol for designing siRNAs with high functionality and specificity. *Nat. Protoc.* **2007**, *2*, 2068–2078. [CrossRef] [PubMed]
54. Altschul, S.F.; Madden, T.L.; Schäffer, A.A.; Zhang, J.; Zhang, Z.; Miller, W.; Lipman, D.J. Gapped BLAST and PSI-BLAST: A new generation of protein database search programs. *Nucleic Acids Res.* **1997**, *25*, 3389–3402. [CrossRef]
55. Petri, S.; Meister, G. siRNA design principles and off-target effects. *Methods Mol. Biol.* **2013**, *986*, 59–71. [CrossRef]
56. Corman, V.M.; Müller, M.A.; Costabel, U.; Timm, J.; Binger, T.; Meyer, B.; Kreher, P.; Lattwein, E.; Eschbach-Bludau, M.; Nitsche, A.; et al. Assays for laboratory confirmation of novel human coronavirus (hCoV-EMC) infections. *Eurosurveillance* **2012**, *17*, 20334. [CrossRef] [PubMed]
57. Shehata, M.M.; Mostafa, A.; Teubner, L.; Mahmoud, S.H.; Kandeil, A.; Elshesheny, R.; Boubak, T.A.; Frantz, R.; Pietra, L.L.; Pleschka, S.; et al. Bacterial Outer Membrane Vesicles (OMVs)-Based Dual Vaccine for Influenza A H1N1 Virus and MERS-CoV. *Vaccines* **2019**, *7*, 46. [CrossRef] [PubMed]
58. Reusken, C.B.; Ababneh, M.; Raj, V.S.; Meyer, B.; Eljarah, A.; Abutarbush, S.; Godeke, G.-J.; Bestebroer, T.M.; Zutt, I.; Müller, M.A. Middle East Respiratory Syndrome coronavirus (MERS-CoV) serology in major livestock species in an affected region in Jordan, June to September 2013. *Eurosurveillance* **2013**, *18*, 20662. [CrossRef] [PubMed]
59. Hemida, M.G.; Perera, R.A.; Wang, P.; Alhammadi, M.A.; Siu, L.Y.; Li, M.; Poon, L.L.; Saif, L.; Alnaeem, A.; Peiris, M. Middle East Respiratory Syndrome (MERS) coronavirus seroprevalence in domestic livestock in Saudi Arabia, 2010 to 2013. *Eurosurveillance* **2013**, *18*, 20659. [CrossRef]
60. Mostafa, A.; Kandeil, A.; Shehata, M.; El Shesheny, R.; Samy, A.M.; Kayali, G.; Ali, M.A. Middle East Respiratory Syndrome Coronavirus (MERS-CoV): State of the Science. *Microorganisms* **2020**, *8*, 991. [CrossRef]
61. Baharoon, S.; Memish, Z.A. MERS-CoV as an emerging respiratory illness: A review of prevention methods. *Travel Med. Infect. Dis.* **2019**, *32*, 101520. [CrossRef]
62. Shehata, M.M.; Gomaa, M.R.; Ali, M.A.; Kayali, G. Middle East respiratory syndrome coronavirus: A comprehensive review. *Front. Med.* **2016**, *10*, 120–136. [CrossRef] [PubMed]
63. Zhang, Z.; Shen, L.; Gu, X. Evolutionary dynamics of MERS-CoV: Potential recombination, positive selection and transmission. *Sci. Rep.* **2016**, *6*, 1–10. [CrossRef] [PubMed]
64. Raj, V.S.; Mou, H.; Smits, S.L.; Dekkers, D.H.W.; Müller, M.A.; Dijkman, R.; Muth, D.; Demmers, J.A.A.; Zaki, A.; Fouchier, R.A.M. Dipeptidyl peptidase 4 is a functional receptor for the emerging human coronavirus-EMC. *Nature* **2013**, *495*, 251–254. [CrossRef] [PubMed]
65. Kandeil, A.; Gomaa, M.; Shehata, M.; El-Taweel, A.; Kayed, A.E.; Abiadh, A.; Jrijer, J.; Moatasim, Y.; Kutkat, O.; Bagato, O.; et al. Middle East respiratory syndrome coronavirus infection in non-camelid domestic mammals. *Emerg. Microbes Infect.* **2019**, *8*, 103–108. [CrossRef] [PubMed]
66. Kandeil, A.; Gomaa, M.; Nageh, A.; Shehata, M.M.; Kayed, A.E.; Sabir, J.S.M.; Abiadh, A.; Jrijer, J.; Amr, Z.; Said, M.A.; et al. Middle East Respiratory Syndrome Coronavirus (MERS-CoV) in Dromedary Camels in Africa and Middle East. *Viruses* **2019**, *11*, 717. [CrossRef]
67. Sayed, A.S.; Malek, S.S.; Abushahba, M.F. Seroprevalence of Middle East Respiratory Syndrome Corona Virus in dromedaries and their traders in upper Egypt. *J. Infect. Dev. Ctries.* **2020**, *14*, 191–198. [CrossRef]
68. Müller, M.A.; Meyer, B.; Corman, V.M.; Al-Masri, M.; Turkestani, A.; Ritz, D.; Sieberg, A.; Aldabbagh, S.; Bosch, B.J.; Lattwein, E.; et al. Presence of Middle East respiratory syndrome coronavirus antibodies in Saudi Arabia: A nationwide, cross-sectional, serological study. *Lancet Infect. Dis.* **2015**, *15*, 559–564. [CrossRef]
69. Sikkema, R.S.; Farag, E.A.B.A.; Himatt, S.; Ibrahim, A.K.; Al-Romaihi, H.; Al-Marri, S.A.; Al-Thani, M.; El-Sayed, A.M.; Al-Hajri, M.; Haagmans, B.L.; et al. Risk Factors for Primary Middle East Respiratory Syndrome Coronavirus Infection in Camel Workers in Qatar During 2013–2014: A Case-Control Study. *J. Infect. Dis.* **2017**, *215*, 1702–1705. [CrossRef]

70. WHO. *Middle East Respiratory Syndrome Coronavirus (MERS-CoV), Fact Sheet*; WHO: Geneva, Switzerland, 2022.
71. Al-Tawfiq, J.A.; Memish, Z.A. Update on therapeutic options for Middle East Respiratory Syndrome Coronavirus (MERS-CoV). *Expert Rev. Anti Infect. Ther.* **2017**, *15*, 269–275. [CrossRef]
72. Friedrich, M.; Aigner, A. Therapeutic siRNA: State-of-the-Art and Future Perspectives. *BioDrugs* **2022**, *36*, 549–571. [CrossRef]
73. Shawan, M.M.A.K.; Sharma, A.R.; Bhattacharya, M.; Mallik, B.; Akhter, F.; Shakil, M.S.; Hossain, M.M.; Banik, S.; Lee, S.-S.; Hasan, M.A.; et al. Designing an effective therapeutic siRNA to silence RdRp gene of SARS-CoV-2. *Infect. Genet. Evol.* **2021**, *93*, 104951. [CrossRef] [PubMed]
74. Yang, Y.; Zhang, L.; Geng, H.; Deng, Y.; Huang, B.; Guo, Y.; Zhao, Z.; Tan, W. The structural and accessory proteins M, ORF 4a, ORF 4b, and ORF 5 of Middle East respiratory syndrome coronavirus (MERS-CoV) are potent interferon antagonists. *Protein Cell* **2013**, *4*, 951–961. [CrossRef] [PubMed]
75. Sohrab, S.S.; Aly El-Kafrawy, S.; Mirza, Z.; Hassan, A.M.; Alsaqaf, F.; Azhar, E.I. In silico prediction and experimental validation of siRNAs targeting ORF1ab of MERS-CoV in Vero cell line. *Saudi J. Biol. Sci.* **2021**, *28*, 1348–1355. [CrossRef] [PubMed]
76. Sohrab, S.S.; El-Kafrawy, S.A.; Mirza, Z.; Hassan, A.M.; Alsaqaf, F.; Azhar, E.I. Designing and evaluation of MERS-CoV siRNAs in HEK-293 cell line. *J. Infect. Public Health* **2021**, *14*, 238–243. [CrossRef] [PubMed]